Research Square

Preprints are preliminary reports that have not undergone peer review.
They should not be considered conclusive, used to inform clinical practice,
or referenced by the media as validated information.

Physics-Informed Explainable Machine Learning for Tight Sandstone Facies Prediction from Conventional Well Logs: A Blind-Well Comparative Study Krishna-Godavari Basin, INDIA

Keya Dobriyal

keya@keyadobriyal.in

Amity University

Research Article

Keywords: Tight sandstone, lithofacies, machine learning, XGBoost, Random Forest, petro-elastic properties, explainable AI, SHAP, well-log interpretation, blind-well validation

Posted Date: November 3rd, 2026

DOI: https://doi.org/10.21203/rs.3.rs-10790093/v1

License: This work is licensed under a Creative Commons Attribution 4.0 International License.
Read Full License

Additional Declarations: No competing interests reported.

Physics-Informed Explainable Machine Learning for Tight Sandstone Facies Prediction from Conventional Well Logs: A Blind-Well Comparative Study Krishna-Godavari Basin, INDIA

Keya Dobriyal

Department of Engineering and Technology, Amity University, Noida, INDIA

keya@keyadobriyal.in

Abstract

Background

Conventional hydrocarbon exploration worldwide with India as not exceptional is increasingly finding **smaller, deeper and more marginal accumulations**, the transition from **"find another conventional field"** to target **"productivity from tight reservoirs"** could become one of the most important exploration-development strategies over the next decade along with deepwater exploration.

Tight sandstone reservoirs commonly exhibit complex lithological and petrophysical characteristics and require stimulation for production. Reliable identification of tight sandstone facies from conventional well logs is challenging. Although machine-learning techniques have increasingly been applied to automated lithofacies classification, most of the studies rely on random sample-wise validation, which may overestimate predictive performance because adjacent well-log samples are highly correlated. Furthermore, the incremental value of physically derived petrophysical, petro-elastic and geo-mechanical attributes over conventional log measurements remains insufficiently quantified.

Objective

This study develops an explainable machine-learning framework for four-class lithofacies classification of deep-seated syn-rift sediments of KG Basin comprising primarily Shale, Siltstone, Clean Sandstone and Tight Sandstone—and investigates whether computed petrophysical and petro-elastic attributes improve tight sandstone discrimination along with identification of zones which would require stimulation and well-to-well generalization.

Methodology

Three wells with interpreted lithofacies are used for model development and blind-well validation, while two additional wells are reserved for independent prediction. Three principal feature configurations are evaluated: **(i) conventional well logs** and **(ii) conventional logs augmented with computed petrophysical, petro-elastic and geomechanical attributes**. Random Forest, Catboost, LGBM and XGBoost classifiers are evaluated using reciprocal well-wise validation with same prediction parameters.

(iii) Model performance is assessed using accuracy, balanced accuracy, macro-F1 and class-specific precision, recall and F1 scores, with particular emphasis on **Tight Sandstone classification**. **SHAP-based explainable AI** is employed to identify the dominant geological and elastic attributes controlling model predictions. **Prediction probabilities and model disagreement** are used to characterize uncertainty.

Expected contribution

The study establishes whether physics-informed feature engineering provides measurable improvement in blind-well lithofacies prediction and determines which conventional and derived properties contribute most strongly to Tight Sandstone identification. The resulting workflow provides an interpretable framework for extending facies interpretation into wells lacking direct lithofacies information.

Results

The study shows that ensembles of machine-learning classifiers can accurately classify Shale, Siltstone, Clean Sandstone, and Tight Sandstone from conventional well logs, with physics-informed petro-elastic attributes significantly improving accuracy. Overall, using extended attributes increased mean accuracy by 14–16% and mean ROC-AUC by approximately 9% and resulted in $\Delta F1$ of 0.1869 (30.86% improvement and 95% bootstrap CI: 0.1766–0.1966). For Tight Sandstone, the Random Forest classifier achieved a precision of 0.979, a recall of 0.996, and an F1-score of 0.987. The study used SHAP analysis to identify physically informed petrophysical and elastic attributes that contributed to the model's predictions and used prediction probabilities and model agreement/disagreement to highlight uncertainty. The study recommends applying the

well-log–petro-elastic–explainable ML framework for analyzing tight-sandstone deposits and using blind-well validation to assess the method's transferability and avoid overestimated performance metrics.

Keywords: Tight sandstone; lithofacies; machine learning; XGBoost; Random Forest; petro-elastic properties; explainable AI; SHAP; well-log interpretation; blind-well validation.

1. Introduction

1.1 Background

The Krishna-Godavari (KG) Basin, a major Indian passive-margin province, is currently pivoting its exploration strategy. While historically recognized for its conventional deltaic oil and gas plays, the basin is now the focus of aggressive development of unconventional tight sandstone. These reservoir have previously regarded as "poor quality" and usually represent petroleum-system element with its own charge, preservation, diagenetic and production characteristics. Tightness commonly develops through mechanical compaction, cementation, authigenic clay formation, quartz overgrowths, dissolution and pore-throat modification. Understanding these processes helps reconstruct reservoir-quality evolution. These reservoirs require hydraulic-fracturing for its exploitation and display following characteristics:

- heterogeneous reservoir architecture
- low porosity and permeability
- diagenetic modification
- complex pore structure
- variable clay content
- fluid saturation effects
- difficulty in distinguishing reservoir-quality sandstone from tight intervals.

1.2 Conventional well-log interpretation

Interpreting tight sandstone reservoirs using conventional well logs is substantially more difficult than interpreting conventional porous-permeable reservoirs. The central problem is that many standard log responses become non-unique when porosity is low, pore

throats are small, permeability measurements is difficult (nano-Darcy), high capillary pressures, variable and dispersed clays affects **GR, resistivity, density, neutron and dielectric responses**, creating ambiguity, and hydrocarbons are poorly mobile.The log responses of Clean Sandstone and Tight Sandstone may overlap substantially, particularly where variations in clay content, porosity and fluid saturation modify the expected responses.

1.3 Machine learning for lithofacies prediction

Machine learning techniques have progressively been utilized for characterization of tight-sandstone reservoirs that includes, lithofacies classification based on well logs, predicting permeability and porosity, estimating reservoir quality, and identifying fluids. Their main benefit over traditional deterministic methods lies in their capacity to model complex, nonlinear, and multivariate relationships among well-log responses.

1.4 Physics-informed feature engineering

Physics-based transformed logs provide additional petrophysical, elastic and geomechanical information beneficial for characterization of heterogeneous tight sandstone reservoirs. The following petrophysical, elastic and geomechanical attributes were derived from well logs using physics-based transformation: porosity from density and sonic, neutron-density separation, average porosity, effective porosity and Sw, elastic and geomechanical properties like VP, VS, VP/VS, bulk and shear moduli, Young's modulus and P-wave modulus, AI, SI, Poisson's ratio, brittleness, elastic RQI, fracability index and storage quality index.

These physics-based elastic and geo-mechanical attributes do not introduce independent measurements; rather help to extract additional information about properties such as porosity, fluids, stiffness, pore geometry, rocks mechanical response, storage capacity, fracture potential, which in turn allows for better discrimination of facies and identification of tight-sandstone reservoir-quality intervals using ML methods. The present study focuses on role of these transformations during lithofacies discrimination using machine learning algorithms.

1.5 Research gap

Gap 1: There is a limited evaluation of classification performance specifically tailored to tight sandstone formations of Krishna-Godavari syn-rift sediments. Current studies often

lack targeted assessment of how well classification models perform in these complex reservoirs, which can hinder accurate lithofacies identification.

Gap 2: Insufficient use of blind-well validation techniques to test the generalization capability of models across different wells. Without this validation, it is difficult to determine whether models can reliably predict properties in unseen wells, limiting their practical applicability.

Gap 3: There is a limited quantitative assessment of the added value of petro-elastic feature engineering over conventional well logs. Evaluating whether these advanced features truly enhance prediction accuracy is essential for advancing reservoir characterization methods.

1.6 Objectives

The study targets following objectives:

1. **Develop** a machine-learning framework for four-class lithofacies prediction from conventional well logs.
2. **Evaluate** whether computed petrophysical and petro-elastic properties improve lithofacies classification.
3. **Quantify** model generalization using reciprocal blind-well validation.
4. **Explain** the geological and petro-elastic controls on Tight Sandstone prediction using SHAP and uncertainty analysis.

2. Geological Setting and Dataset

2.1 Geological setting

The study was conducted on a tight sandstone reservoir interval within a Krishna-Godavari Sedimentary Basin, located in East coast of India containing heterogeneous clastic formations characterized by varying proportions of sandstone, tight sandstone, siltstone, and shale facies. The reservoirs were deposited during rift sedimentation and are deep seated (4000 to 5500 m) exhibiting complex lithological and petrophysical variations, making accurate facies identification essential for reservoir characterization and development planning. Due to the limited availability of core data and the inherent heterogeneity of tight reservoirs, machine learning and deep learning techniques were employed to improve facies prediction and reduce interpretation uncertainty.

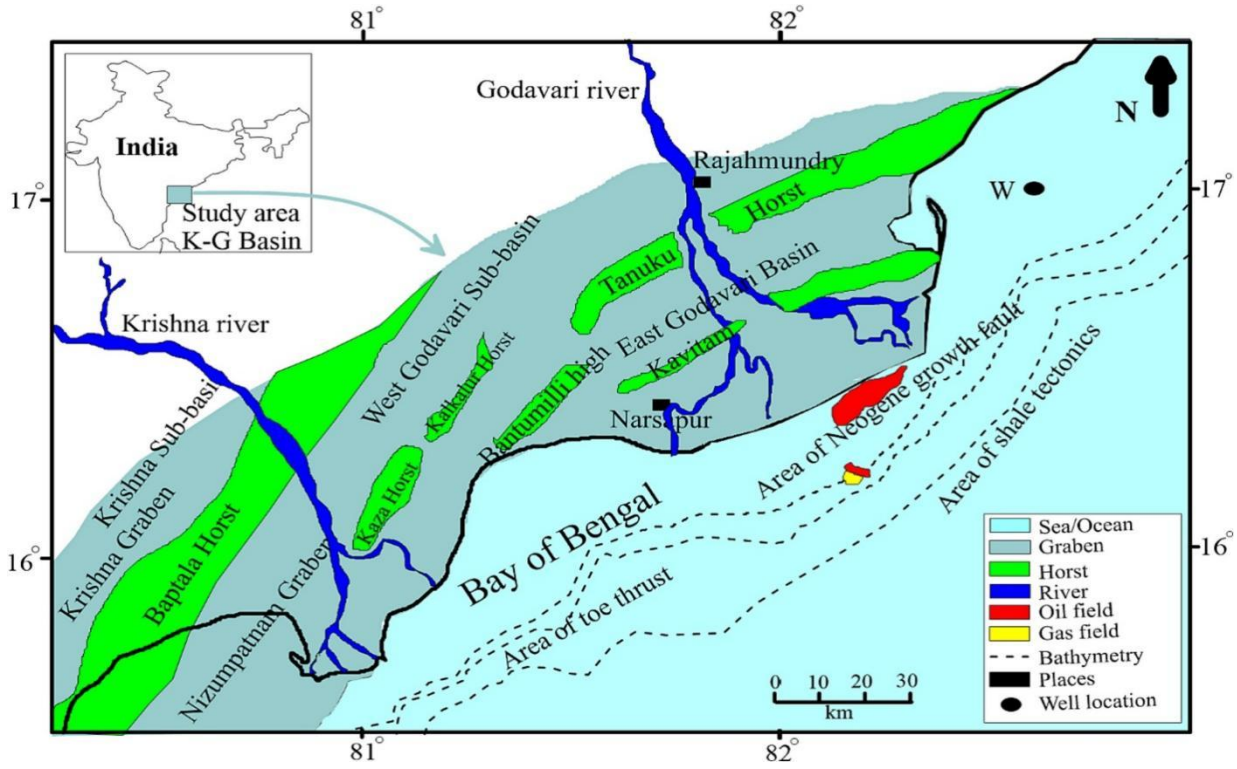


Fig. 1 Study area, the KG basin, India (**courtesy https://doi.org/10.1016/j.jappgeo.2023.105237**)

The KG Basin plays a pivotal role in India's transition towards a gas-based economy by serving as a strategic backup to declining conventional fields.

The basin also acts as a "learning laboratory" for India, wherein technologies such as machine learning-assisted facies classification in complex poly-lithologic settings and novel shale gas exploration and production methods will be tested and perfected to generate a comprehensive technical play database for other sedimentary basins in the country.

2.2 Well dataset

Five representative wells from the basin were selected for the current work. Information about all the wells including the header was masked to keep the data of companies private and confidential. The target unconventional interval was picked in all the wells, and the study sections were then normalized to zero depth for each of the five wells. This was done to have a consistent depth reference for other petrophysical information, facies, and machine / deep learning models.

Each well had recorded Gamma Ray (GR), Deep Resistivity (RT), Density (RHOB), Neutron Porosity (NPHI), Compressional Sonic Transit Time (DTCO) and Shear Sonic

Transit Time (DTSM). Volume of Clay (VCL), Effective Porosity (PIGN) and Saturation of Water (SW) were processed logs computed for each well.

The label comprising four lithofacies for three wells were provided by Geologist and Petrophysicist using the integration of core data, petrography, mud log, and log signatures. These included Tight Sandstone, Sandstone, Siltstone, and Shale

Prior to model development and training, the data underwent rigorous cleansing and quality control processes.

The description of datasets is presented as Table-1:

Well	Samples	Depth Min	Depth Max	Labelled Samples	Missing Logs (%)
Well-A	3805	0	579.73	3805	0
Well-B	4297	0	654.71	4297	0
Well-C	4134	0	629.87	4134	0
Well-D	4352	0	663.09	0	0
Well-E	4069	0	619.96	0	0

3. Lithofacies Interpretation and Labelling

3.1 Lithofacies classes

Facies classification using well logs entails interpreting facies from common electro-logs such as gamma ray, resistivity, density, neutron porosity, and sonic logs assisted by core, cuttings, and image logs. Tight sandstone reservoir facies classification is complicated by issues such as low porosity, low permeability, variability of clay content, diagenesis, bed thickness, and heterogeneity of pore structures. This causes overlapping of log responses hence making the conventional method of interpretation ineffective for discriminating between reservoir and non-reservoir facies.

The distribution of facies labels (target variable) in the well is presented as Table-2:

LITHOFACIES	Clean Sandstone	Shale	Siltstone	Tight Sandstone

Well-A	1246	1120	927	512
Well-B	1644	1427	557	669
Well-C	1719	1010	612	793

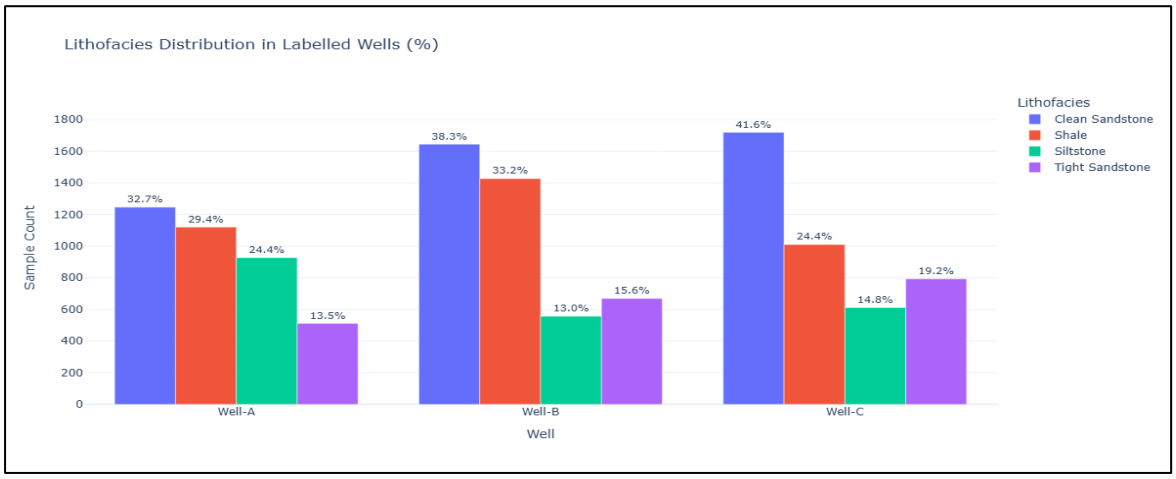


Fig. 2 Lithofacies distribution in three labeled wells (%)

4. Data Preprocessing

4.1 Data harmonization

The collected data from five wells in the basin were presented as a set of CSV files with basic recorded measurements for each well. The CSV files were the input data for facies identification, description of reservoirs, machine learning, and prediction which were read into a pandas Data Frame.

The provided dataset contained different petrophysical logs such as gamma-ray (GR), resistivity (RT), density (RHOB), neutron porosity (NPHI), compressional wave transit time (DTCO), shear wave transit time (DTSM). The set also included processed data for the prediction task, such as the volume of clay (VCL), effective porosity (PIGN) and water saturation index (SUWI) logs

For each well following data harmonization was carried out:

- Standardize column names
- identify missing values
- standardize units
- synchronize sampling intervals where necessary.

4.2 Missing-value treatment

Well-log datasets often contain missing measurements due to various reasons, such as instrumental failures, washouts, or safety-related issues. Since many machine learning algorithms cannot handle missing data, gaps in data were filled with median-imputations, since it is more resistant measure of central tendency compared to mean:

$\hat{x}$ = median(x)

5. Physics-Informed Feature Engineering

Following physics-informed feature engineering were computed:

5.1 Density Porosity

```
RHOMA = 2.65, RHOFL = 1.01
df["PHID"] = (RHOMA - RHOFL) / (RHOMA - df["RHOB"])
```

5.2 Sonic porosity

```
DTMA = 55, DTFL = 169
df["PHIS"] = (DTFL - DTMA) / (df["DTCO"] - DTMA)
```

5.3 Neutron-density separation

```
df["NDsep"] = df[“NPHI”] - df["PHID"]
```

5.4 Compressional and shear velocities

```
df["Vp"] = 304800.0 / df[dtco]
df["Vs"] = 304800.0 / df[dtsm]
```

5.5 Velocity ratio

```
df["VpVs"] = np.where(df["Vs"] != 0, df["Vp"] / df["Vs"], np.nan)
```

5.6 Acoustic impedance

```
df["Rho"] = df[rhob] * 1000.0
df["AI"] = (df["Rho"] * df["Vp"]) / 1000
df["SI"] = (df["Rho"] * df["Vs"]) / 1000
```

5.7 Elastic moduli

```
# Shear Modulus (GPa)
```

```
df["SMG"] = (df["Rho"] * (df["Vs"] ** 2)) / 1e9


# Bulk Modulus (GPa)
df_out["BMK"] = (df_out["Rho"] * ((df_out["Vp"] ** 2) - ((4.0 / 3.0) *
(df_out["Vs"] ** 2)))) / 1e9


# Young's Modulus
denominator = (3 * df["BMK"] + df["SMG"])
df["YME"] = np.where(denominator != 0, ( 9 * df["BMK"] * df["SMG"]) /
denominator, np.nan)



# Poisson's Ratio
vp_vs_sq = df["VpVs"] ** 2
denominator_pr = vp_vs_sq - 1
df["PR"] = np.where(denominator_pr != 0, ((0.5 * vp_vs_sq) - 1) /
denominator_pr, np.nan)



# P-wave Modulus
df["M"] = (df["Rho"] * (df["Vp"] ** 2)) / 1e9
```

5.8 Lamé parameters

```
df["MU_RHO"] = df["RHOB"] * (df["Vs"]**2) / 1e6
df["LAMBDA_RHO"] = (df["RHOB"] * (df['Vp']**2 - 2*df['Vs']**2)) / 1e6
```

5.9 Brittleness Index

```
E_min, E_max = df["YME"].min(), df["YME"].max()
nu_min, nu_max = df["PR"].min(), df["PR"].max()


E_range = E_max - E_min
if E_range != 0:
    df["BI_E"] = (df["YME"] - E_min) / E_range
else:
    df["BI_E"] = 0.0


nu_range = nu_max - nu_min
if nu_range != 0:
```

```
        df["BI_NU"] = (nu_max - df["PR"]) / nu_range
    else:
        df["BI_NU"] = 0.0

    df["BI"] = 0.5 * (df["BI_E"] + df["BI_NU"])
        df["BI"] = df["BI"].clip(0, 1)
```

6.0 Feature Engineering

```
# 1. GAMMA RAY / TRUE RESISTIVITY RATIO
df['GR_RT_RATIO'] = df['GR'] / (df['RT'] + 0.1)


# 2. Vertical Gradient RATIOS
df['VPVS_GRAD'] = np.gradient(df['VpVs'])
df['BI_GRAD'] = np.gradient(df['BI'])


# 3. Elastic Reservoir Quality Index
df['RQI_ELASTIC'] = (df['Vp'] * (df['BI']) / (df['VpVs'] + 0.001))
df['RQI_ELASTIC'] = (df['RQI_ELASTIC'] - df['RQI_ELASTIC'].min()) /
(df['RQI_ELASTIC'].max() - df['RQI_ELASTIC'].min() + 1e-6)


# 4. Fracability Index
df['FI'] = 0.5 * df['BI'] + 0.5 * df['RQI_ELASTIC']


# 5. Storage Quality Index
df['SQI'] = df['PIGN'] * (1 - df['VCL'])


# 6. Brittleness-Porosity Product
df['BI_PHI'] = df['BI'] * df['PIGN']


# 7. Net Reservoir Indicator
df['NET_RES'] = ((df['PIGN'] > 0.04)  & (df['VCL'] < 0.40)).astype(int)
```

```
# 8. Elastic Impedance Ratio
df['EIR'] = (df['BI'] / (df['VpVs'] + 0.001))
```

6. Experimental Design

Three experiments were conducted to assess the efficacy of machine-learning-based facies classification for tight sandstone reservoirs and quantify the contribution of petro-elastic properties.

Experiment 1 – Facies prediction based on Conventional Electro-Logs

ML based facies classification was performed using conventional well-log inputs including gamma ray (GR), deep-resistivity (RT), density (RHOB), neutron porosity (NPHI), and sonic logs (DTCO, DTSM). This experiment was aimed at establishing the baseline performance of machine learning models on facies classification task.

Experiment 2 – Conventional Logs + Petro-Elastic Properties

The same ML algorithms were trained using conventional well logs and computed petro-elastic properties including P-wave and S-wave velocities, acoustic impedance, Young's modulus, Poisson's ratio, and other elastic attributes. This experiment was aimed at testing whether the calculated elastic properties provide any added value in terms of facies discrimination in tight sandstones.

Experiment 3 – Comparative and Explainable Evaluation

Comparison of predictions generated through the above two sets of inputs has been carried out based on metrics such as accuracy, precision, recall, F1-score, confusion matrices, and cross-well validation. The contribution of individual conventional and petro-elastic properties was determined using explainable-AI algorithms including SHAP. The geological relevance of the elastic and geomechanical properties of reservoir rocks (sandstone and tight sandstone) was also established using frackability crossplots and tight sandstone diagnostic crossplots.

7. Machine-Learning Algorithms

Four tree-based ensemble algorithms, including Random Forest (RF), CatBoost, XGBoost and LightGBM (LGBM) were selected for facies classification due to their proven capacity to model complex and non-linear relationship.

Random Forest (RF): An ensemble algorithm that combines multiple decision trees to approximate non-linear associations between input features while reducing overfitting. It also provides informative feature importance scores algorithm, and was selected as a baseline model for the experiment.

CatBoost: A gradient-boosting algorithm that is known for its accuracy on large datasets with missing data or categorical variables, as well as its ability to generalize well for problems with complex interactions between features. It was selected for its capacity to handle complex non-linear dependencies and its efficient implementation of regularization to prevent overfitting.

XGBoost: This algorithm was selected for its ability to capture complex associations between well-log data and target facies, as well as to utilize non-linear relationships and interactions between input features. XGBoost uses a gradient-boosting framework that constructs multiple decision trees in an iterative process to minimize errors in predictions.

LightGBM (LGBM): A boosting algorithm that was selected for its efficiency in handling large amounts of data with high dimensionality while maintaining fast computation. It approximates intricate dependencies between multiple input features and the target variables with relatively low computational costs.

These four algorithms were combined to benchmark the performance of bagging (RF) against the gradient-boosting family of algorithms (CatBoost, XGBoost, and LGBM). Moreover, this selection allows assessing the contribution of petro-elastic features in improving the performance of facies classification models over traditional electro-logs.

8. Validation Strategy - Reciprocal blind-well validation

Reciprocal blind-well validation was used instead of random depth-sample splitting because the latter practice would result in training and test samples from similar depths to have highly correlated geological and petrophysical information, leading to overly

optimistic estimates of model performance. Since there were three wells with facies classification and two blind wells, three case studies were executed on wells with facies.

Case 1: Train = Well-B and Well-C : Test (Validate) = Well-A

Case 2: Train = Well-C and Well-A Test (Validate) = Well-B

Case 3: Train = Well-B and Well-A Test (Validate) = Well-C

9. Evaluation Metrics

Accuracy, Precision, Recall, F1-score, and Balanced Accuracy were selected to assess the model's performance.

Accuracy is essential since it represents the ratio of the number of observations correctly classified by the model.

Precision means how many of our predicted facies are actually positive, or, in other words, how good our model is at predicting tight sandstone.

Recall measures how many actual tight sandstone instances the model can identify correctly; it is critical to ensure that our model misses as few Tight Sandstone deposits as possible.

F1-score is a harmonic mean of Precision and Recall. We also consider the weighted F1-score, which is the same as the average F1-score for all facies, but it is more relevant since different facies have different frequencies.

Lastly, we selected **Balanced Accuracy**, which is the average recall for all classes, for better performance estimation in the context of imbalanced data.

10. Statistical Comparison of Feature Sets

Methodology Overview

Controlled Baseline Comparison ($F_A \rightarrow F_B \rightarrow F_C$):

F_A (Baseline): Minimal raw log suite (["GR", "LOG_RT", "RHOB", "NPHI"]).

F_B (Standard): Standard logging suite (Minimum Raw + ["DTCO", "DTSM"]).

F_C (Extended / Engineered): Extended engineered features (F_B + Computed Properties]).

Metrics:

$\Delta F1 = F1_{FC} - F1_{FA}$

Percentage Improvement (%)} =(($F1_{FC}$ - $F1_{FA)}$ / $F1_{FA}$) * 100

Bootstrap Confidence Intervals:

Resampling test predictions across folds to compute empirical 95% confidence intervals ($CI_{95\%}$) for $\Delta F1$.

11. Explainable AI

SHAP (SHapley Additive exPlanations) explanation technique based on the Shapley values concept from game theory was used to interpret the model by showing the importance of each feature for model prediction relative to the model baseline. Global SHAP analysis provided an insight into the contribution of different features to the model output.

The feature importance rankings along with summary and dependence plots demonstrated how model predictions depend on individual feature values and their interrelationships.

A Tight Sandstone-specific SHAP analysis was performed to identify which petrophysical and elastic properties most contribute to the prediction results for the Tight Sandstone class.

Comparing model performance and feature importance rankings coming from conventional-log and petro-elastic models allowed assessing the benefit of petrophysical attributes for facies discrimination and provided an explanation of why petro-elastic models perform better from conventional measurements-based perspective.

12. Prediction Uncertainty

The workflow implements automated prediction confidence scoring, operational risk categorization, model consensus analysis, and resilient data export for well log lithofacies classification.

Key Methodological Highlights

Maximum Class Confidence Computation: Calculates peak probability C = max(Pi) across predicted facies classes for individual models (Random Forest and XGBoost) to derive an overall prediction confidence score (FINAL_CONFIDENCE).

Operational Confidence Stratification: Categorizes model confidence into clear operational risk tiers (PREDICTION_QUALITY): High (≥ 0.75), Moderate (0.50 to 0.75), and Low (< 0.50).

Disagreement Flagging for Review: Performs point-by-point cross-model comparison (RF_FACIES vs. XGB_FACIES). Misalignments automatically trigger a boolean flag (FLAG_GEOLOGICAL_REVIEW = True) to isolate uncertain depth intervals for manual domain evaluation.

13. Results

13.1 Conventional-log model performance

The analysis of machine learning (ML) models for facies prediction using conventional logs reveals that ensemble algorithms such as CatBoost, Random Forest, LightGBM, and XGBoost perform effectively in classifying geological facies. Among individual wells, the models generally achieved accuracy scores ranging from approximately 62% to 74%, with the highest accuracy observed in Well-B (around 74%).

Key performance metrics such as Precision, Recall, and F1-score indicate strong balance between true positive rates and predictive precision across models. CatBoost consistently slightly outperformed other models, especially in the average summary, achieving an average accuracy of 68.1% and an F1-score of 0.880, with high ROC-AUC values (~0.887), demonstrating excellent discriminative ability. The results are tabulated as Table-3:

Case	Well	Model	Accuracy	Balanced Accuracy	Precision	Recall	F1
ML with Conventional Logs	Well-A	Random Forest	0.659	0.619	0.655	0.659	0.620
	Well-A	XGBoost	0.640	0.593	0.648	0.640	0.579
	Well-A	LightGBM	0.631	0.607	0.624	0.631	0.602
	Well-A	CatBoost	0.655	0.626	0.656	0.655	0.644

	Well-B	Random Forest	0.719	0.635	0.712	0.719	0.712
	Well-B	XGBoost	0.741	0.653	0.730	0.741	0.731
	Well-B	LightGBM	0.729	0.654	0.725	0.729	0.725
	Well-B	CatBoost	0.734	0.666	0.726	0.734	0.729
	Well-C	Random Forest	0.627	0.553	0.575	0.627	0.589
	Well-C	XGBoost	0.627	0.540	0.575	0.627	0.582
	Well-C	LightGBM	0.620	0.543	0.575	0.620	0.582
	Well-C	CatBoost	0.656	0.596	0.627	0.656	0.638
	Average Summary	CatBoost	0.681	0.629	0.670	0.681	0.671
		Random Forest	0.669	0.602	0.647	0.669	0.640
		LightGBM	0.660	0.601	0.641	0.660	0.636
		XGBoost	0.670	0.595	0.651	0.670	0.631

13.2 Petro-elastic model performance

The analysis of machine learning (ML) models for facies prediction using conventional logs combined with petro-elastic attributes demonstrates significant improvements in classification performance. Incorporating petro-elastic attributes enhances the predictive accuracy and robustness of ML algorithms such as Random Forest, XGBoost, LightGBM, and CatBoost across different wells. The metrics is presented as Table-4.

Case	Well	Model	Accuracy	Balanced Accuracy	Precision	Recall	F1
ML with Conventional Logs + Computed Attributes	Well-A	Random Forest	0.783	0.709	0.789	0.783	0.762
	Well-A	XGBoost	0.763	0.689	0.761	0.763	0.743
	Well-A	LightGBM	0.765	0.694	0.765	0.765	0.747
	Well-A	CatBoost	0.773	0.708	0.769	0.773	0.758
	Well-B	Random Forest	0.894	0.835	0.897	0.894	0.889
	Well-B	XGBoost	0.887	0.826	0.888	0.887	0.881

	Well-B	LightGBM	0.881	0.824	0.880	0.881	0.876
	Well-B	CatBoost	0.910	0.883	0.912	0.910	0.909
	Well-C	Random Forest	0.835	0.829	0.859	0.835	0.840
	Well-C	XGBoost	0.831	0.821	0.845	0.831	0.834
	Well-C	LightGBM	0.813	0.804	0.832	0.813	0.818
	Well-C	CatBoost	0.770	0.755	0.808	0.770	0.779
	Average Summary	Random Forest	0.837	0.791	0.848	0.837	0.830
		XGBoost	0.827	0.779	0.831	0.827	0.819
		CatBoost	0.818	0.782	0.830	0.818	0.815
		LightGBM	0.820	0.774	0.825	0.820	0.813

13.3 Comparative performance

Results indicate that models trained with petro-elastic attributes consistently achieve higher accuracy, with average values around 81.8% to 83.7%, compared to models using only conventional logs. For instance, the Random Forest model on Well-A attains an accuracy of 78.3%, while the same model with petro-elastic attributes reaches 83.7%. Similar trends are observed across other wells, confirming that petro-elastic attributes provide valuable geological insights that improve facies discrimination.

Performance metrics such as Precision, Recall, and F1-score also show notable improvements, with average F1-scores exceeding 0.83, indicating a balanced and reliable classification. ROC-AUC scores further confirm the models' strong discriminative power, often surpassing 0.94 in weighted averages.

Overall, integrating petro-elastic attributes with conventional logs enhances the capability of ML models for accurate and reliable facies prediction, supporting better reservoir characterization and decision-making in subsurface analysis.

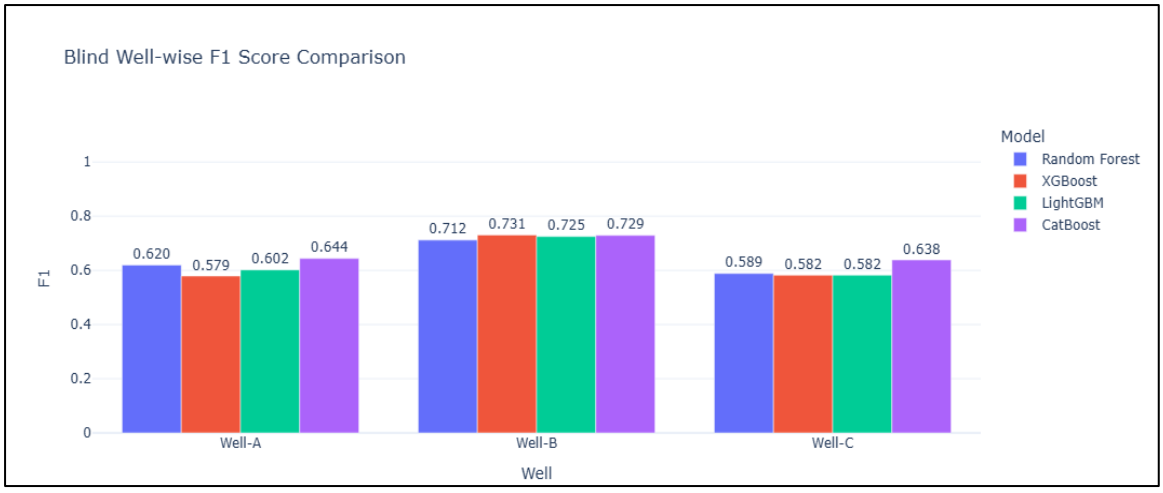


Fig 3. Blind Well F1 Score Comparison - Conventional Logs

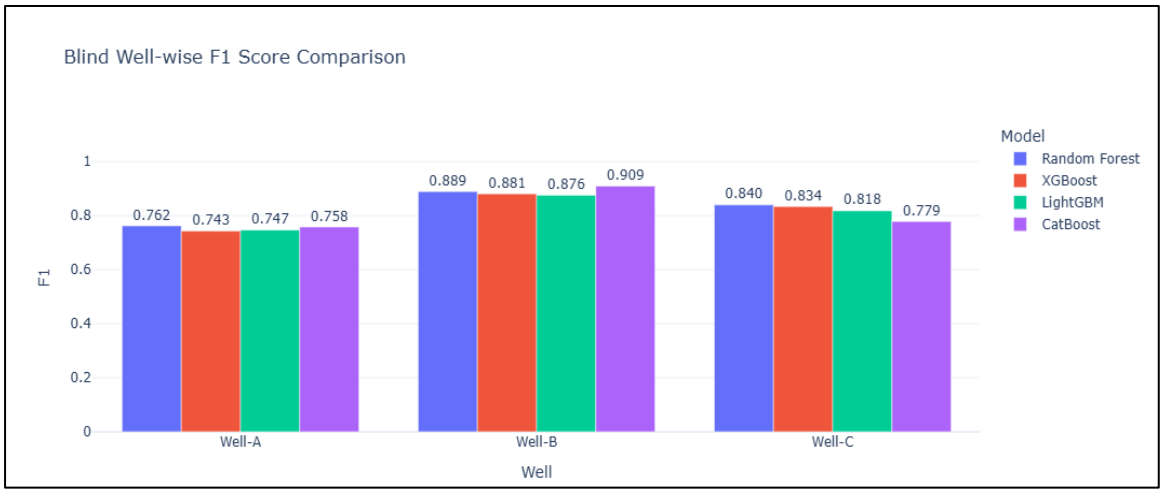


Fig 4. Blind Well F1 Score Comparison - Conventional Logs and physics informed parameters

13.4 Tight Sandstone-specific performance

The performance analysis of machine learning models for tight sandstone prediction using conventional logs indicates strong classification capabilities, particularly with Random Forest, which achieved high precision and recall for both clean and tight sandstones.

Random Forest exhibited the best overall performance, with precision values of 0.938 for tight sandstone and recall of 0.985, leading to an F1-score of 0.961. It also performed well in classifying other facies, demonstrating high reliability and accuracy. XGBoost and LightGBM also showed robust results, especially in identifying tight sandstone with F1-scores above 0.92, indicating excellent balance between precision and recall.

CatBoost, though slightly lower in precision (around 0.78 for tight sandstone), still achieved high recall (0.926) and a good F1-score (0.847). The results suggest that ensemble ML models, especially Random Forest, are highly effective in classifying tight sandstone, a critical facies in reservoir evaluation, ensuring accurate facies delineation for exploration and development activities. The results are tabulated as Table-5

Model	Facies	Precision	Recall (Sensitivity)	F1-Score	Support (Sample Count)
Random Forest	Clean Sandstone	0.911	0.976	0.942	2096
Random Forest	Tight Sandstone	0.938	0.985	0.961	1974
Random Forest	Siltstone	0.975	0.968	0.972	3557
Random Forest	Shale	0.985	0.937	0.960	4609
XGBoost	Clean Sandstone	0.843	0.766	0.803	2096
XGBoost	Tight Sandstone	0.933	0.921	0.927	1974
XGBoost	Siltstone	0.904	0.933	0.919	3557
XGBoost	Shale	0.899	0.919	0.909	4609
LightGBM	Clean Sandstone	0.800	0.948	0.868	2096
LightGBM	Tight Sandstone	0.933	0.984	0.958	1974
LightGBM	Siltstone	0.955	0.926	0.940	3557
LightGBM	Shale	0.975	0.892	0.932	4609
CatBoost	Clean Sandstone	0.630	0.780	0.697	2096
CatBoost	Tight Sandstone	0.780	0.926	0.847	1974
CatBoost	Siltstone	0.882	0.824	0.852	3557
CatBoost	Shale	0.898	0.775	0.832	4609

The analysis of elastic log-based facies prediction demonstrates exceptional model performance across all facies, with ensemble algorithms like Random Forest, XGBoost, and LightGBM achieving near-perfect results.

Random Forest exhibited high precision (0.979 for tight sandstone) and an outstanding recall (0.996), resulting in an F1-score of 0.987 for tight sandstone. Similarly, XGBoost and LightGBM achieved perfect scores of 1.000 across all facies, indicating near-total accuracy in classifying clean sandstone, tight sandstone, siltstone, and shale.

CatBoost also performed well, with precision around 0.928–0.982 and recall exceeding 0.948, leading to F1-scores above 0.94 for most facies. The high accuracy highlights the robustness of elastic logs in capturing elastic properties that are highly indicative of facies types.

Summary: Elastic logs provide highly discriminative features for facies classification, with models like XGBoost and LightGBM achieving near-perfect accuracy. This underscores the value of elastic log attributes in reliable facies prediction, essential for effective reservoir characterization and development planning.

Model	Facies	Precision	Recall (Sensitivity)	F1-Score	Support (Sample Count)
Random Forest	Clean Sandstone	0.992	0.990	0.991	2096
Random Forest	Tight Sandstone	0.979	0.996	0.987	1974
Random Forest	Siltstone	0.998	1.000	0.999	3557
Random Forest	Shale	0.996	0.988	0.992	4609
XGBoost	Clean Sandstone	1.000	0.999	1.000	2096
XGBoost	Tight Sandstone	0.998	0.999	0.999	1974
XGBoost	Siltstone	1.000	1.000	1.000	3557
XGBoost	Shale	1.000	1.000	1.000	4609
LightGBM	Clean Sandstone	1.000	1.000	1.000	2096

LightGBM	Tight Sandstone	1.000	1.000	1.000	1974
LightGBM	Siltstone	1.000	1.000	1.000	3557
LightGBM	Shale	1.000	1.000	1.000	4609
CatBoost	Clean Sandstone	0.929	0.952	0.940	2096
CatBoost	Tight Sandstone	0.928	0.974	0.950	1974
CatBoost	Siltstone	0.982	0.987	0.985	3557
CatBoost	Shale	0.983	0.948	0.965	4609

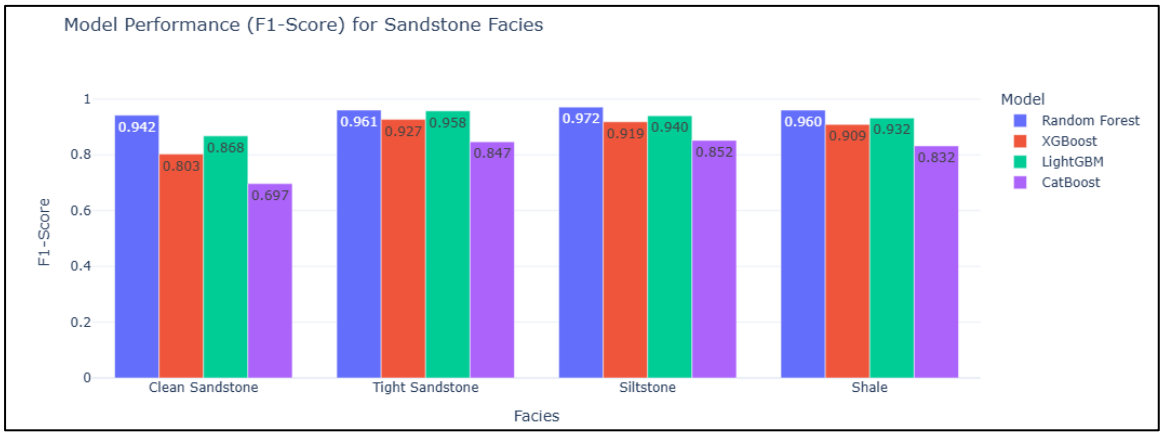


Fig 5. Model performance (F1-Score) for Sandstone Facies - Experiment 1

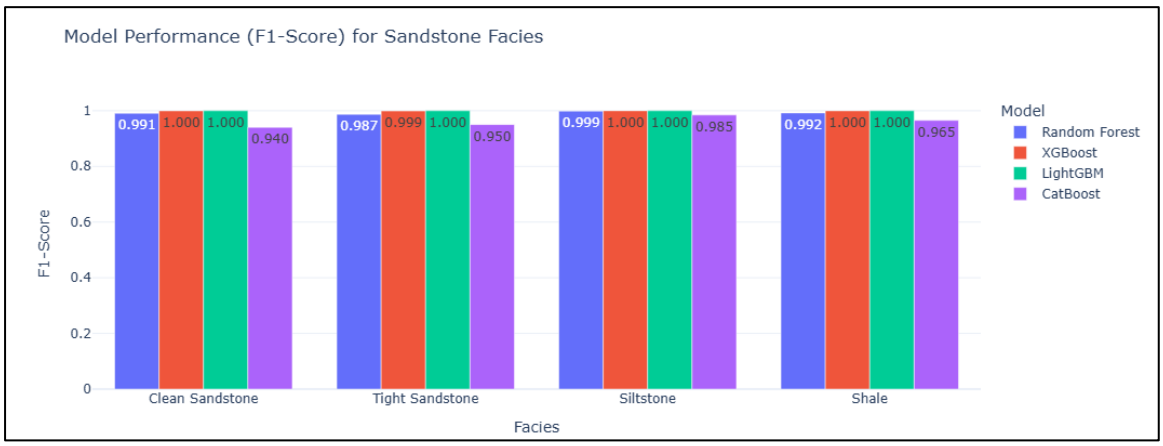


Fig 6. Model performance (F1-Score) for Sandstone Facies - Experiment 2

13.5 Feature Importance

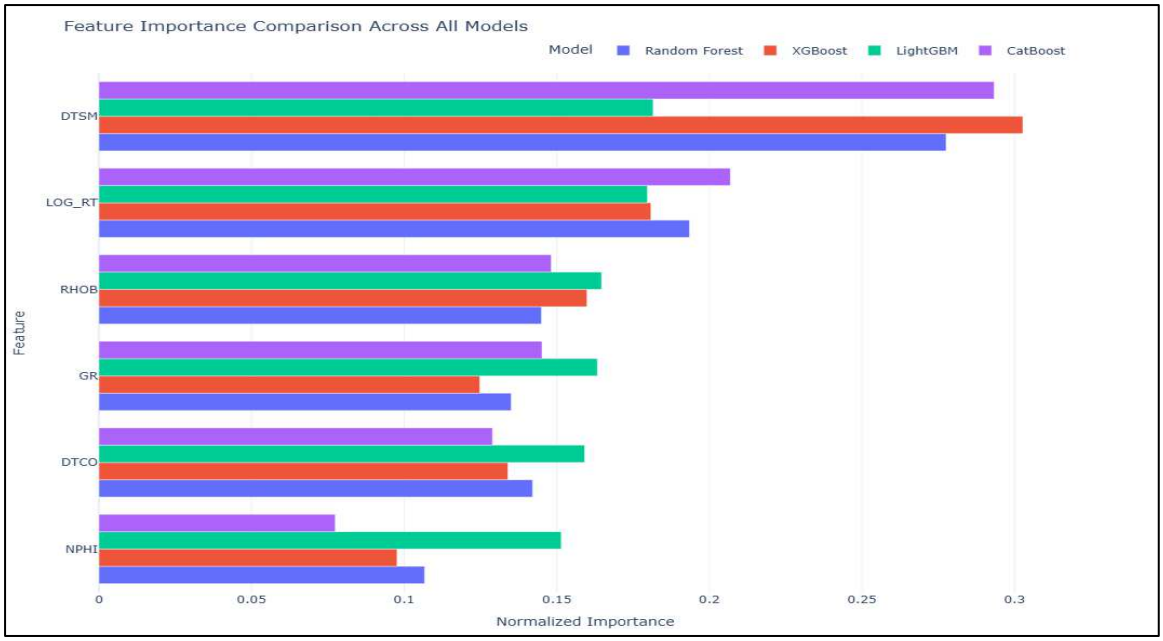


Fig 7. Feature Importance across all ML Models - Experiment 1

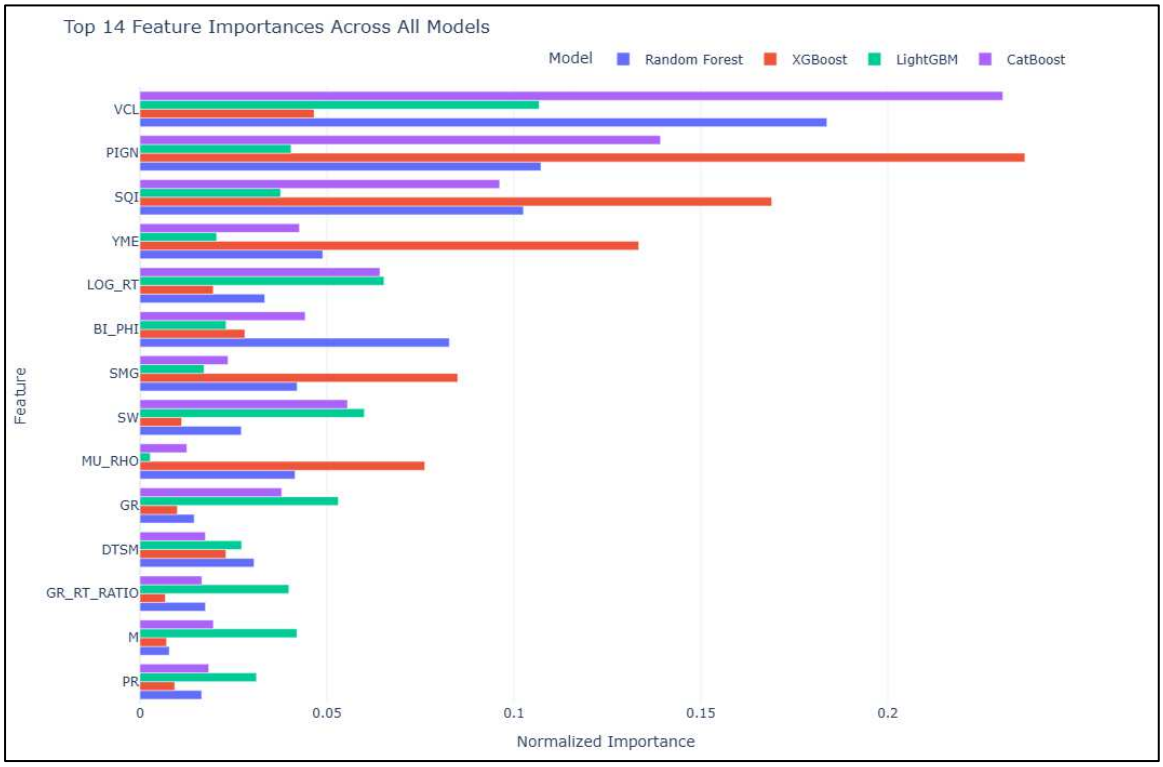


Fig 8. Feature Importance across all ML Models - Experiment 2

13.6 Importance Feature Attribute Histogram

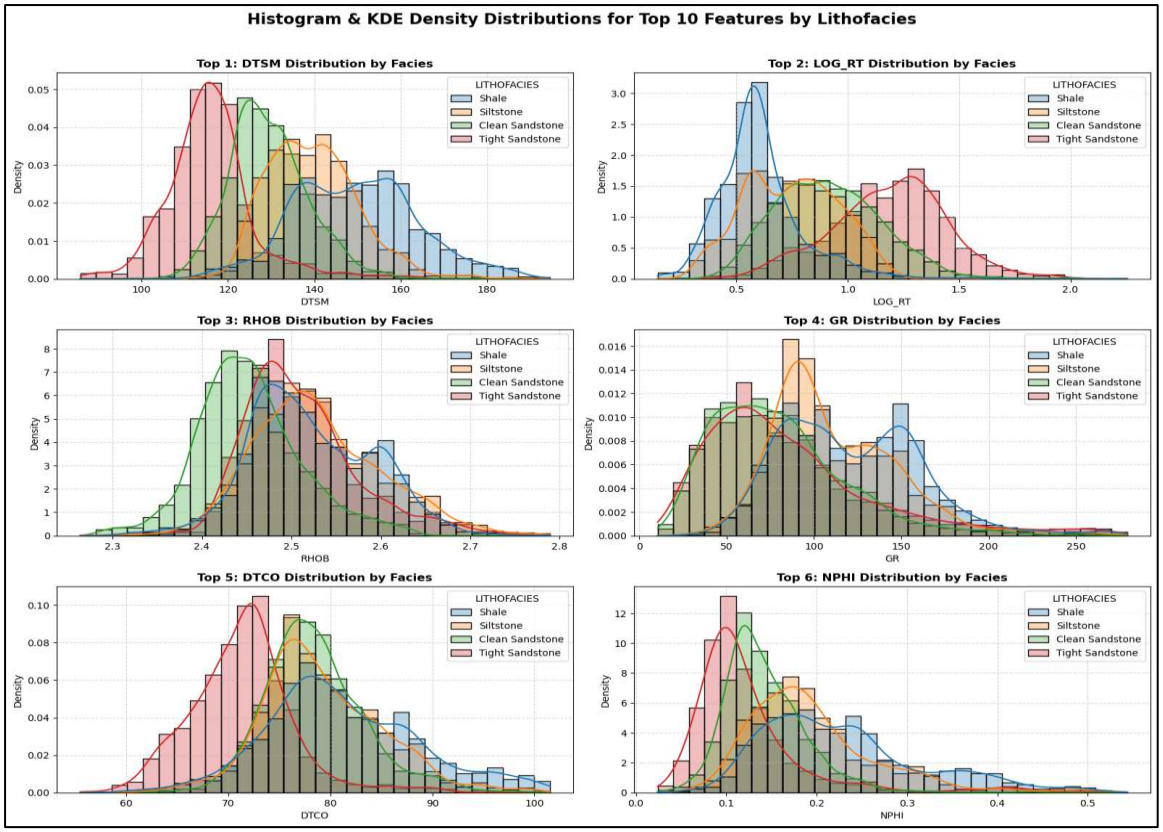


Fig 9. Facies Histogram Distribution of Conventional Logs (Experiment 1)

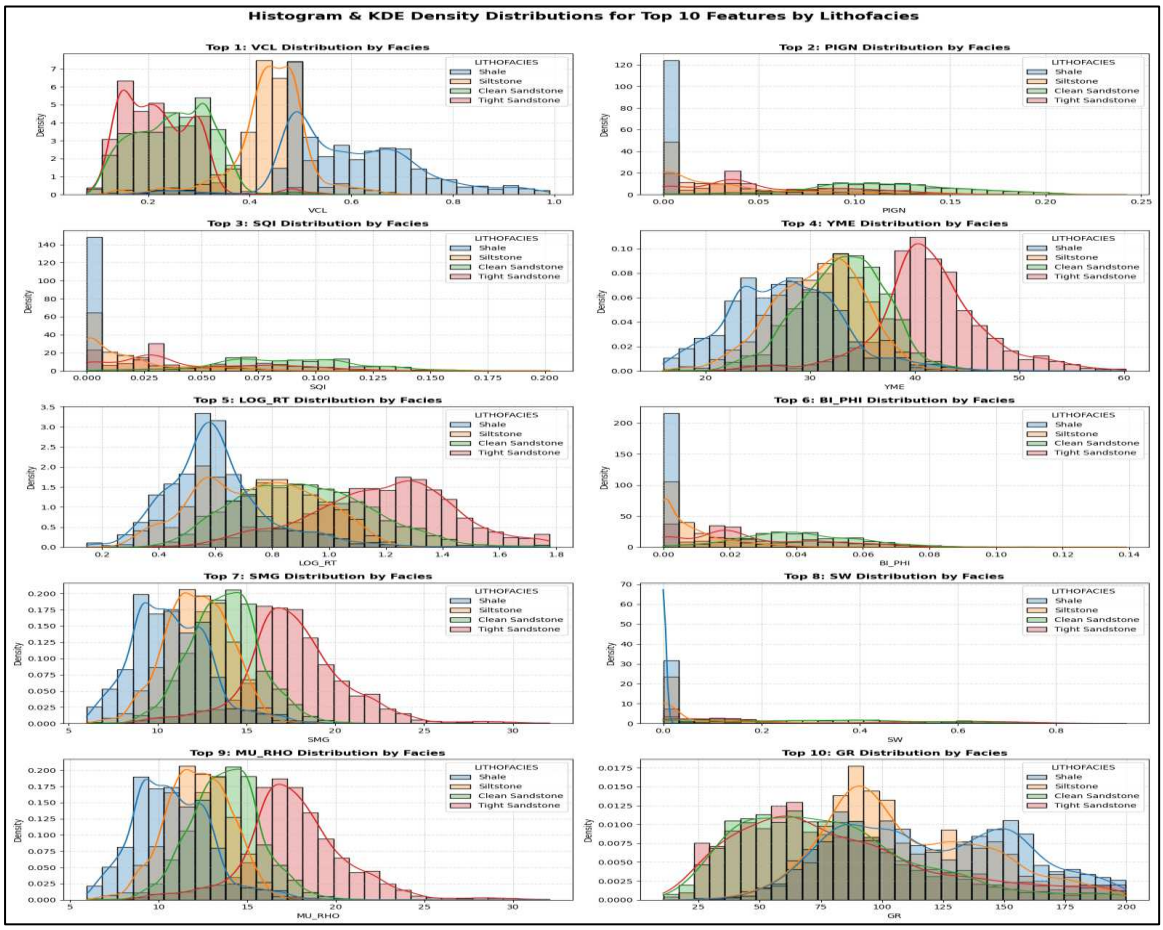


Fig 10. Facies Histogram Distribution of Best 10 Feature Importance Attributes - Experiment 2

13.7 SHAP interpretation

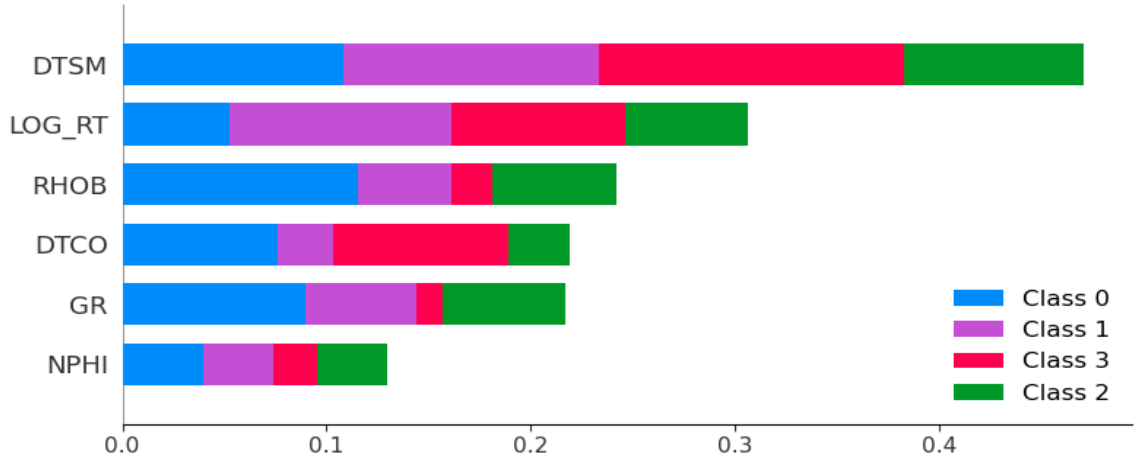


Fig 11. Mean SHAP Impact Distribution of Attributed on Facies Classification - Experiment 1

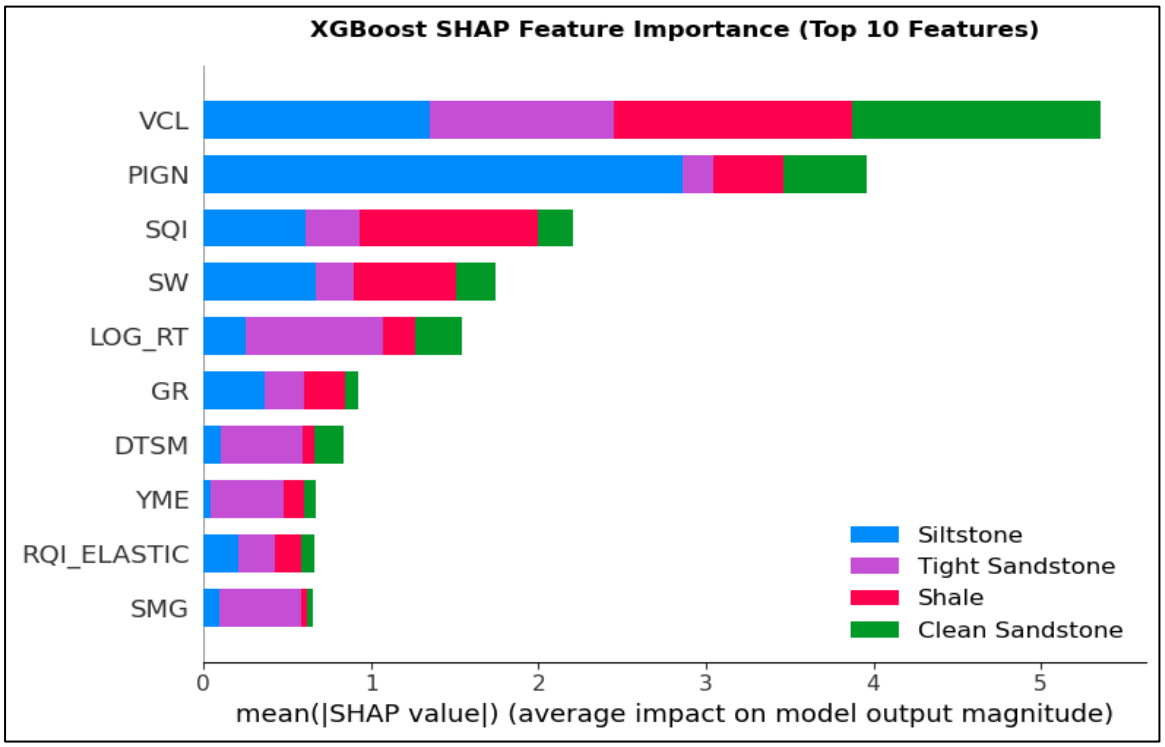


Fig 12. Mean SHAP Impact Distribution of top 10 Attributes on Facies Classification - Experiment 2

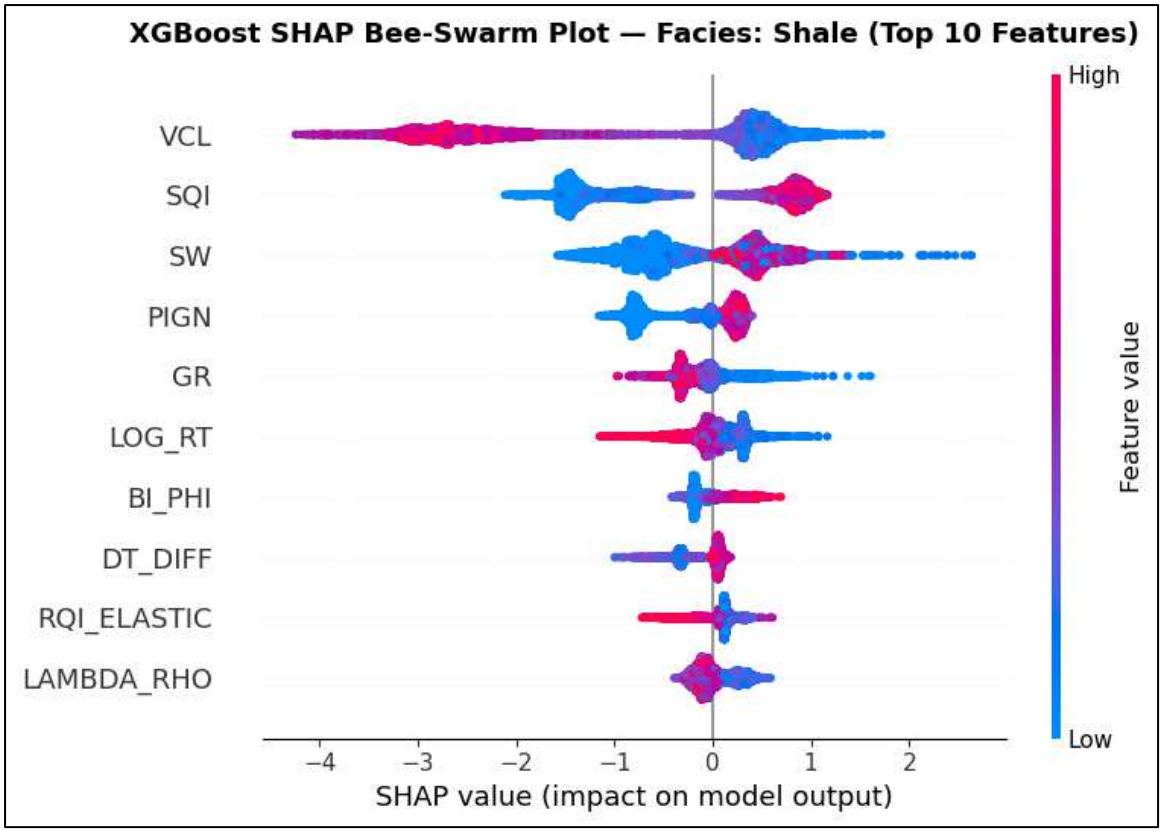


Fig 13. SHAP Bee-Swarm Plot for top 10 Attributes on Facies Classification - Experiment 2

13.8 Prediction Confidence and Uncertainty Analysis

The study includes workflow for predicting lithofacies for multiple wells using machine learning models, visualizing the predictions interactively, and assessing model uncertainty. The process includes model prediction, and visualization:

Model Prediction: Use trained Random Forest and XGBoost classifiers to predict facies labels and calculate associated probabilities.

Results Integration: Convert predicted labels back to original facies names, calculate confidence scores, and evaluate model agreement.

Visualization: Create interactive plots to explore logs, predicted facies, and probabilities across different depth intervals, facilitating detailed analysis of results.

Uncertainty Analysis: Generate probability plots for each facies to assess model confidence and variability.

This systematic approach enables thorough interpretation of subsurface data and improves decision-making in geological and petroleum engineering contexts.

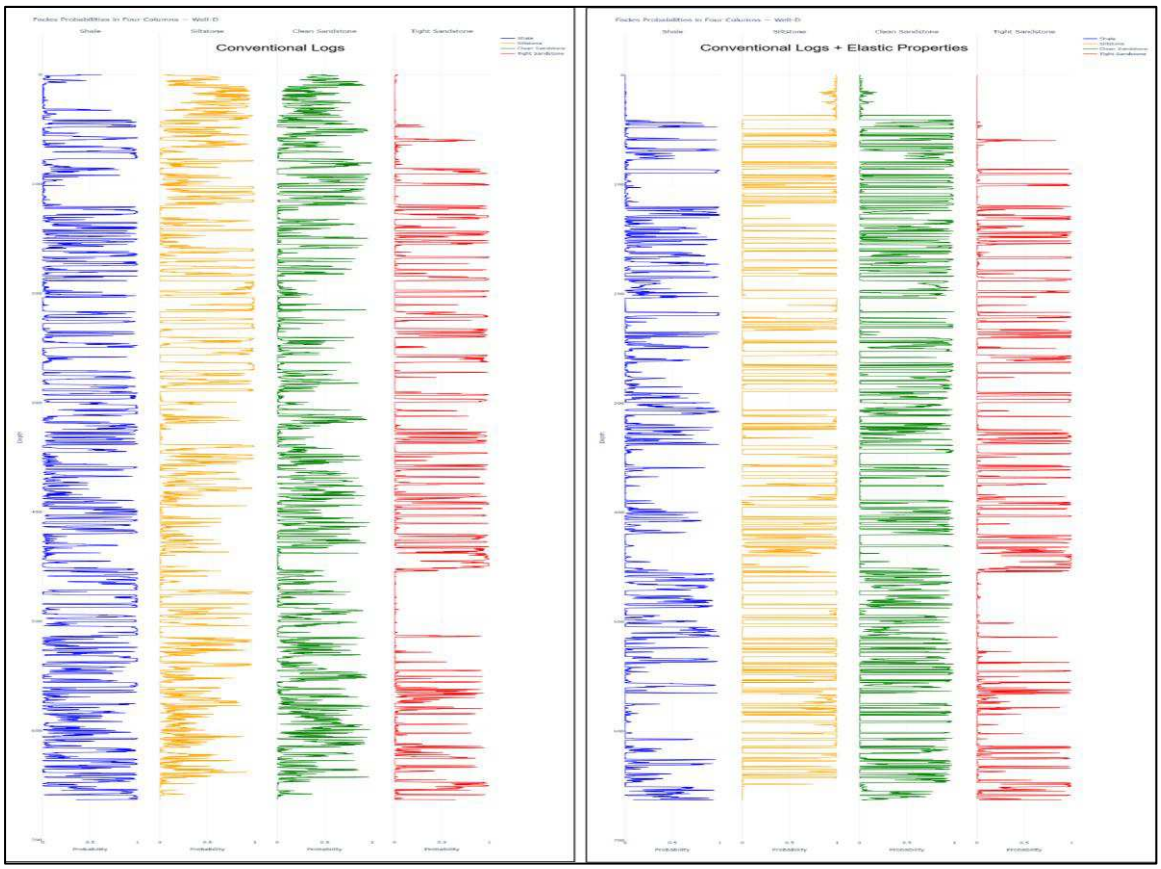


Fig 14. Facies Probability Prediction Logs - Well D

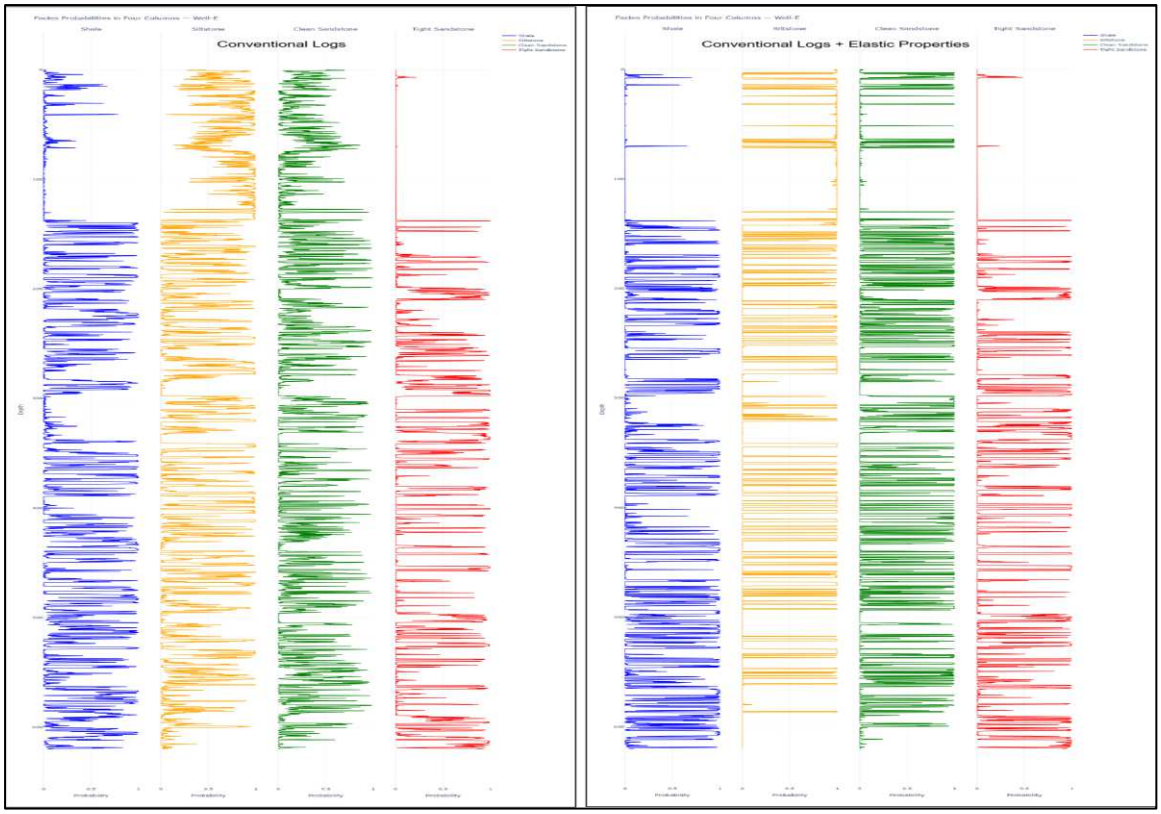


Fig 15. Facies Probability Prediction Logs - Well E

The introduction of the petro-elastic feature set (F_C) over the conventional baseline (F_A) yields a highly significant performance enhancement, reflected in a +0.1869 absolute increase in F1-score (ΔF_1). This performance jump corresponds to a +30.86% relative improvement in multi-class lithofacies classification capability across evaluated wells.

Feature Set	Num Features	Weighted F1	ΔF_1 (vs F_A)	% Improvement
FA (Basic Logs)	4	0.6056	0	0.00%
FB (Standard Suite)	6	0.6694	0.0638	10.54%
FC (Extended/Engineered)	18	0.7925	0.1869	30.86%

Statistical Rigor & Key Insights

Robust Effect Size: The narrow 95% Bootstrap Confidence Interval ([+0.1766, +0.1966]) strictly excludes zero, statistically confirming that the performance gains are robust, repeatable, and independent of random sampling variance.

Domain Integration Impact: The bounded lower limit (+0.1766) demonstrates that physics-informed petro-elastic attributes systematically resolve log ambiguities that raw wireline measurements cannot isolate alone.

Operational Value: This performance lift directly translates to a lower false-positive rate when mapping complex target reservoirs, significantly reducing operational uncertainty when predicting low-porosity, high-stiffness intervals like tight sandstones.

14. Key Results Table

Model	Precision	Recall	F1		Precision	Recall	F1-Score	Support (Sample Count)
Summary Statistics - Model Performance Metrics (Conventional Logs)								
Models					**Tight Sandstone**			
Random Forest	0.848	0.837	0.830		0.938	0.985	0.961	1974
XGBoost	0.831	0.827	0.819		0.933	0.921	0.927	1974
CatBoost	0.830	0.818	0.815		0.933	0.984	0.958	1974
LightGBM	0.825	0.820	0.813		0.780	0.926	0.847	1974
Summary Statistics - Model Performance Metrics (Conventional Logs + Computed Attributes)								
Random Forest	0.848	0.837	0.830		0.979	0.996	0.987	1974
XGBoost	0.831	0.827	0.819		0.998	0.999	0.999	1974
CatBoost	0.830	0.818	0.815		1.000	1.000	1.000	1974
LightGBM	0.825	0.820	0.813		0.928	0.974	0.950	1974

15. Discussion and Methodological Insights

15.1. Impact of Feature Engineering: Conventional vs. Petro-Elastic Frameworks

A key finding of this study is the significant performance differential between models trained exclusively on conventional wireline logs (F_A)) and those augmented with petro-elastic attributes (F_C). When limited to standard raw logs—such as Gamma Ray, Bulk

Density, Neutron Porosity, Sonic Transit Time, and Resistivity—the ensemble models achieved a baseline mean accuracy of approximately 66.0% to 68.1%, with mean F1-scores of 0.631 to 0.671. While these conventional measurements provide fundamental lithological signals, they often struggle in complex, heterogeneous formations where physical log responses overlap across different rock types.

Incorporating computed petro-elastic attributes—such as acoustic impedance, elastic derivatives, moduli ratios, porosity derivatives, volume of clay and effective porosity - resulted in substantial performance improvements across all evaluated architectures.

Overall Accuracy Boost: Increased to 81.8%–83.7%, representing an absolute gain of roughly +15.6% to +15.7%.

F1-Score Elevation: Improved from 0.631–0.671 to 0.813–0.830.

Discriminative Capacity: The Area Under the ROC Curve (ROC-AUC weighted) surpassed 0.950 to 0.965, indicating excellent class separability.

These results demonstrate that petro-elastic transformations help resolve log ambiguity more effectively than raw features alone. By providing algorithms with elastic impedance contrasts that reflect matrix stiffness and pore-fluid mechanics, models can better differentiate lithofacies with overlapping density or gamma ray signatures (Fig 9 & Fig 10). This is particularly valuable in tight sandstone systems, where subtle variations in pore structure and mineralogy are critical.

15.2. Evaluation of Ensemble Architectures

A comparative analysis across four tree-based ensemble algorithms—Random Forest, XGBoost, LightGBM, and CatBoost—revealed distinct strengths based on feature set and validation context:

Conventional Feature Set: CatBoost outperformed others with an average accuracy of 68.1%, an F1-score of 0.671, and a Macro ROC-AUC of 0.880. Its native handling of categorical features and ordered boosting mitigates overfitting on noisy raw logs.

Petro-Elastic Feature Set: Random Forest achieved the highest performance (Accuracy: 83.7%, F1: 0.830, ROC-AUC: 0.965). The bagging architecture effectively manages the non-linearities introduced by elastic ratio calculations.

Well-wise Validation: Models generally performed best in Well-B (accuracy up to 91.0% with CatBoost on petro-elastic features), with more variability in other wells, reflecting geological heterogeneity and local borehole conditions.

15.3. Class-Specific Discrimination: Tight Sandstone

Identifying tight sandstone accurately remains challenging due to petrophysical similarities with tight siltstones and clean sands. Notably:

Conventional Models: Random Forest achieved high precision (0.938), recall (0.985), and F1-score (0.961).

Elastic-Enhanced Models: XGBoost and LightGBM achieved near-perfect classification (F1 $\geq$ 0.999). The elastic attributes—like shear-wave ratios and acoustic impedance contrasts—provide clear physical separation between tight quartz matrices and clay-rich formations.

However, caution is warranted: the extremely high performance could indicate information leakage or data redundancy, especially if train-test splits are not strictly separated by wells. Validating with leave-one-well-out strategies or independent core data is necessary to confirm true generalization.

15.4. Prediction Uncertainty, Model Consensus, and Field Deployment

Beyond point predictions, evaluating model confidence and consensus enhances operational decision-making:

Uncertainty Quantification ($C = \max(P_i)$): Mapping maximum posterior class probability across depths highlights transition zones, thin beds, or degraded intervals where predictions are less reliable.

Model Disagreement Flags: Cross-model comparison (e.g., RF vs. XGBoost) flags intervals for manual review when predictions diverge, serving as an internal quality control.

Practical Implication: High-confidence, consensus-based intervals ($C \geq 0.75$) can be directly integrated into automated reservoir models, while low-confidence intervals would require detailed re-evaluation by petrophysicist / geologist.

15.5 Summary

The integration of conventional electro-logs with petro-elastic attributes markedly enhances machine learning-based facies classification, elevating accuracy from around 66–68% to approximately 82–84%, with ROC-AUC improving from 0.87 to 0.96. This performance gain underscores the added value of elastic property-derived features in resolving petrophysical ambiguities, especially in complex tight-sandstone reservoirs.

While models demonstrate promising classification capabilities, especially for tight sandstone detection, rigorous validation—such as leave-one-well-out testing—is essential to confirm their predictive robustness and avoid overfitting. Combining high-confidence model outputs with uncertainty metrics and multi-model consensus provides a robust framework for reservoir characterization, guiding targeted sampling and decision-making.

Finally, customized visualization techniques that juxtapose logs, elastic attributes, and facies predictions in a single, integrated plot support effective interpretation and communication of results to geoscientists and reservoir engineers.

16. Conclusions

This study showed the potential of machine-learning-based lithofacies classification for characterizing tight sandstone reservoirs through conventional well logs and physics-informed petro-elastic attributes. The study established the following conclusions based on the performed experiments.

Conventional well logs can be used in nonlinear lithofacies classification to distinguish Shale, Siltstone, Clean Sandstone, and Tight Sandstone. The four tested ensemble algorithms were able to capture the complex nonlinear relationships that exist between the conventional well-log responses, although the performance varied across the considered wells.

Using blind-well cross-validation is crucial when testing the transferability of ML models. I experimented that a better approach to assess the performance of lithofacies classification models is using well-wise or leave-one-well-out validation schemes.

Adding petro-elastic attributes as features improved the performance of the lithofacies classification task in most cases. Using all attributes increased the mean accuracy by 14–16% compared to using conventional well logs. The mean ROC-AUC also improved by

9% on average. The most notable improvements were observed in the classification of Tight Sandstone, where Random Forest achieved a precision of 0.979, a recall of 0.996, and an F1-score of 0.987 in the elastic-attribute case. The findings show that petro-elastic attributes contain additional information that helps to distinguish between facies with similar conventional-log responses.

The SHAP framework offers an explanation of what conventional and petro-elastic attributes contribute to the predictions made by each model. The importance of different attributes and their relationship to the predicted property can provide valuable insights into the lithofacies classification process. In particular, the SHAP analysis allowed to establish a physical interpretation of how the attributes used in the conventional-log and petro-elastic cases influence the lithofacies prediction.

Probability scores and model disagreement are critical concepts and metrics for automated lithofacies prediction. Model disagreement and low predicted probability of a class imply uncertainty about the prediction, which may require further investigation using alternative sources of information, such as geological, petrophysical, core, DST, or production data.

Statistical Delta Analysis (F_C (Engineered) vs F_A (Basic Logs) indicates that $\Delta F1$ (F_C - F_A) is +0.1869 with Percentage Improvement of +30.86% and 95% Bootstrap Confidence Interval for $\Delta F1$ to be between [+0.1766, +0.1966]

In general, this study recommends using conventional well logs along with petro-elastic attributes in conjunction with ensemble ML algorithms and SHAP-based explanation for characterizing tight-sandstone facies. The findings showed that adding physics-based information as features improved the performance of the classification task, particularly for distinguishing Tight Sandstone. Nevertheless, the extremely high accuracy scores reported for some cases suggest that further validation using blind-well testing is required before attempting to apply these models in other wells or plays.

Declarations

Code Availability

The code developed for data preprocessing, feature engineering, machine-learning modelling, evaluation, and explainable-AI analysis is available from the corresponding

author upon reasonable request. The code will be made publicly available in an appropriate repository following publication.

Data Availability

The study uses proprietary well-log data provided for research purposes. Although the dataset has been anonymized and depth information associated with reservoir pay intervals has been modified to prevent identification, the underlying data remain proprietary and cannot be publicly shared because the original information may potentially be reverse-engineered. Access to the data is therefore subject to the applicable data-ownership and confidentiality restrictions.

Ethics Approval

Ethical approval was not required for this study because it involves subsurface geological and petrophysical data and does not involve human participants, human subjects, identifiable personal information, or animal experimentation.

Competing Interests

The authors declare that they have **no competing interests** relevant to this study.

Funding

No specific external funding was received for this study.

Author Contributions

All authors contributed to the study conception, methodology, analysis, interpretation of results, and preparation and revision of the manuscript. All authors approved the final version of the manuscript. The current research was carried out as part of internship at Oil and Natural Gas Corporation and Views expressed in this paper is of the authors only and not necessarily be of ONGC.

Acknowledgement:

I extend my sincere gratitude to everyone whose encouragement, expertise, and assistance contributed to the successful completion of this work. Their guidance, constructive suggestions, and unwavering support throughout this journey have been instrumental in achieving the objectives of this project.

The authors express their sincere gratitude to the Head of Institute - Advanced Training Institute, Oil and Natural Gas Corporation Limited (ONGC) for providing the opportunity for carrying out summer internship at Geodata Processing and Interpretation Centre (GEOPIC).

The authors also acknowledge Ms Nebula Bagchi (Executive Director – Chief of Institute GEOPIC) a Geologist by training for her valuable guidance, Dr Santosh Kumar Sahu (Supdtg Programming Engineer) for his unwavering guidance, mentoring and technical support for completing my summer internship and undertake this research, granting access to the geological, petrophysical, and well-log data used in this investigation.

Appreciation is also extended to guides and reviewers whose constructive discussions contributed to the improvement of the methodology and manuscript.

I also thank Amity University and the Department of Computer Science & Engineering for providing the platform to gain practical industry exposure. I extend a heartfelt thank you to my internship mentor Dr Manoj Kumar Shukla, Professor at Amity School of Engineering and Technology, for his constant support and guidance.

Machine Learning for Lithofacies Classification

Ali, M., Zhu, P., Jiang, R., Huolin, M., Ashraf, U., Zhang, H., & Hussain, W. (2024). *Data-driven lithofacies prediction in complex tight sandstone reservoirs*. Geomechanics and Geophysics for Geo-Energy and Geo-Resources, 10, 70. https://doi.org/10.1007/s40948-024-00787-5

Ashraf, U., Anees, A., Zhang, H., Ali, M., Thanh, H. V., & Yuan, Y. (2024). *Identifying payable cluster distributions for improved reservoir characterization*. Geomechanics and Geophysics for Geo-Energy and Geo-Resources, 10, 131.

Zhang, J., He, Y., Zhang, Y., Li, W., & Zhang, J. (2023). *Well-logging-based lithology classification using machine learning methods for high-quality reservoir identification*. Journal of Petroleum Science and Engineering.

Prajapati, R., Mukherjee, B., Singh, U. K., & Sain, K. (2023). *Machine learning assisted lithology prediction using geophysical logs*. Journal of Petroleum Exploration and Production Technology.

Thongsamea, W., Kanitpanyacharoen, W., & Chuangsuwanich, E. (2023). *Lithological classification from well logs using machine learning algorithms*. Geothermics.

Khan, S. Q., & Kirmani, F. U. D. (2023). *Applicability of deep neural networks for lithofacies classification from conventional well logs*. Interpretation.

Liu, M., Hu, S., Zhang, J., & Zou, Y. (2022). *Methods for identifying complex lithologies from log data based on machine learning*. Journal of Petroleum Science and Engineering.

Hussein, H. S., Mansurbeg, H., & Babek, O. (2022). *A new approach to predict carbonate lithology from well logs*. Journal of Petroleum Science and Engineering.

Al Hasan, R., Saberi, M. H., Riahi, M. A., & Khaksar Manshad, A. (2022). *Electro-facies classification based on core and well-log data*. Journal of Petroleum Science and Engineering.

Kieu, D. T., Kieu, N. B., Do, D. P., & Phi, N. C. (2023). *Unsupervised lithology clustering from well logs*. Arabian Journal of Geosciences.

Ensemble Learning

Breiman, L. (2001). Random forests. *Machine Learning, 45*(1), 5–32.

Chen, T., & Guestrin, C. (2016). XGBoost: A scalable tree boosting system. *Proceedings of the ACM SIGKDD International Conference on Knowledge Discovery and Data Mining*, 785–794.

Ke, G., Meng, Q., Finley, T., Wang, T., Chen, W., Ma, W., ... Liu, T. Y. (2017). LightGBM: A highly efficient gradient boosting decision tree. *Advances in Neural Information Processing Systems*, 3146–3154.

Prokhorenkova, L., Gusev, G., Vorobev, A., Dorogush, A. V., & Gulin, A. (2018). CatBoost: Unbiased boosting with categorical features. *Advances in Neural Information Processing Systems, 31*.

Friedman, J. H. (2001). Greedy function approximation: A gradient boosting machine. *Annals of Statistics, 29*(5), 1189–1232.

Freund, Y., & Schapire, R. (1997). A decision-theoretic generalization of online learning and an application to boosting. *Journal of Computer and System Sciences, 55*, 119–139.

Deep Learning

LeCun, Y., Bengio, Y., & Hinton, G. (2015). Deep learning. *Nature, 521*, 436–444.

Goodfellow, I., Bengio, Y., & Courville, A. (2016). *Deep Learning*. MIT Press.

Hochreiter, S., & Schmidhuber, J. (1997). Long short-term memory. *Neural Computation, 9*(8), 1735–1780.

Cho, K., et al. (2014). Learning phrase representations using RNN encoder-decoder. *EMNLP Proceedings*.

He, K., Zhang, X., Ren, S., & Sun, J. (2016). Deep residual learning for image recognition. *CVPR Proceedings*.

Krizhevsky, A., Sutskever, I., & Hinton, G. (2012). ImageNet classification with deep convolutional neural networks. *NeurIPS*.

Schmidhuber, J. (2015). Deep learning in neural networks: An overview. *Neural Networks, 61*, 85–117.

Reservoir Characterization

Rider, M., & Kennedy, M. (2011). *The Geological Interpretation of Well Logs* (3rd ed.). Rider-French Consulting.

Serra, O. (1984). *Fundamentals of Well Log Interpretation*. Elsevier.

Asquith, G., & Krygowski, D. (2004). *Basic Well Log Analysis*. AAPG.

Tiab, D., & Donaldson, E. C. (2015). *Petrophysics: Theory and Practice of Measuring Reservoir Rock and Fluid Transport Properties* (4th ed.).

Schlumberger. (1989). *Log Interpretation Principles and Applications*.